IET Generation, Transmission & Distribution

Research Article

Service restoration of active distribution systems with increasing penetration of renewable distributed generation

ISSN 1751-8687
Received on 12th July 2018
Revised 12th January 2019
Accepted on 11th April 2019
doi: 10.1049/iet-gtd.2018.6153
www.ietdl.org

Nikolaos C. Koutsoukis[1], *Pavlos S. Georgilakis*[1] ✉, *Nikos D. Hatziargyriou*[1]
[1]*School of Electrical and Computer Engineering, National Technical University of Athens, Athens, Greece*
✉ *E-mail: pgeorg@power.ece.ntua.gr*

Abstract: The increasing penetration of renewable generation poses several challenges to the operation of distribution networks under emergency conditions. This study proposes a service restoration method that exploits active management of the distribution network. The proposed active network management (ANM) method considers the coordinated control of the available switches, distributed generation, and the operation of on-load tap changer (OLTC) to determine the optimal service restoration plan. The objectives of the proposed model are the minimisation of (i) the out of service area considering customer priorities, (ii) the number of switch operations, (iii) the number of tap changes of the OLTC, and (iv) the injected power from the substations considering the variation of load demand and renewable generation. The service restoration problem is formulated as a mixed-integer second-order cone programming problem, which is efficiently solved by commercial branch and bound solvers. Results on a 135-bus distribution system and a 540-bus distribution system highlight the importance and the benefits of incorporating ANM into the solution of the service restoration problem.

Nomenclature

Sets

T_{out}	duration that the system is at restorative state
$\Omega_{\text{ch}}(i)$	set of the children nodes of bus i
Ω_{cl}	set of distribution lines with normally closed switches
Ω_{L}	set of distribution lines
Ω_{LwS}	set of distribution lines with switches
Ω_N	set of system buses
Ω_{op}	set of distribution lines with normally open switches
Ω_{SS}	set of substation buses
Ω_{OLTC}	set of substations with installed on-load tap changer (OLTC)

Parameters

c_{out}	cost of the non-supplied energy ($/MWh)
c_{sw}	cost of switch operation ($)
$c_{\delta v}$	penalisation cost of voltage deviation ($)
c_{tap}	cost of OLTC operation ($)
c_{ss}	cost of the energy supplied by substation ($/MWh)
M	relatively large number
$P_{d,i,t}/Q_{d,i,t}$	active/reactive load demand of bus i at period t
$P_{dg,i,t}$	active power of the distributed generation (DG) unit of bus i at period t
$P_{\text{DG},i}^{\text{rated}}$	rated active power of the DG unit of bus i
r_{ij}/x_{ij}	resistance/reactance of lines i–j
$S_{\text{DG},i}^{\text{rated}}$	maximum apparent power of the DG inverter at bus i
$S_{\text{lim},ij}$	thermal limit of lines i–j
$S_{\text{SS},i}$	maximum capacity of the substation at bus i
$\text{Step}_{\text{OLTC}}$	step voltage of the OLTC
$\text{tap}_{i,0}$	initial tap position of the OLTC installed at the substation bus i
tap_{max}	maximum number of tap positions of the OLTC
$V_{\text{min}}/V_{\text{max}}$	minimum/maximum voltage magnitude limits
w_i	priority weight factor of customers at bus i
δv^{tr}	threshold limit of voltage relaxation
δ_t	duration of time period t

Variables

$\text{Aux}U_{\text{sqr},i,t}$	auxiliary variable associated with the voltage square magnitude of bus i at period t
$I_{ji,t}^{\text{sqr}}$	square magnitude of current on lines j–i at period t
$P_{ij,t}/Q_{ij,t}$	active/reactive power flow of lines i–j at period t
$P_{\text{ss},i,t}/Q_{\text{ss},i,t}$	active/reactive power injected from substation bus i at period t
$PL_{i,t}/QL_{i,t}$	auxiliary variable associated with the active/reactive power balance at bus i at period t
$Q_{\text{dg},i,t}$	reactive power that is injected by the DG unit of bus i at period t
$\text{tap}_{i,t}^{-}/\text{tap}_{i,t}^{+}$	number of downwards/upwards changes of tap position during the operation of the OLTC of bus i at period t
$U_{i,t}^{\text{sqr}}$	voltage squared magnitude of bus i at period t
$V_{i,t}$	voltage magnitude of bus i at period t
$\delta v_{i,t}^{l}/\delta v_{i,t}^{u}$	relaxation terms of the voltage limits of bus i at period t

Integer variables

$\text{tap}_{i,t}$	tap position of the OLTC installed at the substation bus i at period t

Binary variables

sw_{ij}	switch status of lines i–j. It is equal to 1 if lines i–j is connected; otherwise it is equal to 0
y_{ij}	power flow direction variable. It is equal to 1 if power flows from buses i to j; otherwise, it is equal to 0
$\rho_{i,t}$	connection status of load bus i at period t. It is equal to 1 if a load of bus i at period t is connected to the network; otherwise, it is equal to 0

1 Introduction

Service restoration is one of the fundamental processes in the operation of power distribution networks under emergency conditions [1]. After the location and isolation of a permanent fault, service restoration defines the appropriate operations of the available normally open (NO) and normally closed (NC) switches, to minimise the out of service areas subject to the network's technical constraints. The duration of the fault location, isolation and service restoration process highly depends on the level of distribution automation [2]. Due to the large size of distribution networks, a large number of switching elements, and the network's operational and time constraints, service restoration is a complex and challenging optimisation problem. Furthermore, the increasing penetration of renewable distributed generation (DG) and advancements in communication technologies have created new challenges and opportunities in the operation of distribution networks [3] and the solution of the service restoration problem.

Service restoration can be formulated as a mixed-integer non-linear programming (MINLP) problem due to the non-linearity of the power flow equations and the binary nature of the control variables, i.e. the switches' statuses. A comprehensive review of service restoration models and methods is presented in [4, 5]. In [6], a multi-objective evolutionary algorithm is used to solve the service restoration problem considering the minimisation of the out of service area and the number of switch operations for single and multiple faults. A method based on a genetic algorithm, which determines the optimal switch operations and load shedding strategy, is presented in [7] for distribution network service restoration. A dynamic programming method is used to solve the service restoration method in [8] considering customer priority. Customer priority is also considered in the heuristic method of [9], which employs load curtailment of in-service customers to reduce the switch operations and maintain the network within its operating limits. In [10], service restoration is formulated as a mixed-integer second-order cone programming (MISOCP) problem and it is solved using a commercial branch and bound solver. The objective function of the MISOCP model minimises the switch operations and the number of disconnected load buses, prioritises the remote controlled switches over the manual ones, and considers customer priorities. In [11], the service restoration plan is determined considering the operation of voltage regulation devices of the network. The object-oriented method in [12] considers the load variation during the outage period for the solution of the service restoration problem.

The impact of dispatchable DG on service restoration in balanced and unbalanced distribution networks is examined using the heuristic method of [13]. The two-stage service restoration method in [14] also considers DG in its formulation. In the first stage of [14], a simplified mixed-integer linear programming model defines the statuses of the switches. In the second stage, a nonlinear programming model determines the operating point of the new network topology and the potential disconnection of load buses from the system. A decentralised technique based on expert system rules is utilised in [15] to solve the service restoration problem considering customer priority and DG. Load variation, wind DG, customer priorities, and power supply of the non-faulted areas are incorporated into the restoration method that is based on genetic algorithm in [16] and an expert-based decentralised control strategy in [17].

The service restoration methods in [6–17] aim at determining a temporary network configuration to restore the power supply to the healthy part of the distribution network and do not allow islanded network operation. An alternative approach to minimise the out of service areas during the restoration process is to enable islanded operation of parts of the network powered by distributed energy resources (DERs) [18–21]. In [22–26], the distribution network following a permanent fault is sectionalised into microgrids to restore power supply to critical loads. The service restoration methods in [25, 26] also determine the sequence of DG and ESSs dispatching actions and the switching actions in different time steps during the restoration process. The islanded operation of the network during the restoration process is out of the scope of our paper.

The effect of DG in the elaboration of service restoration plans without resorting to islanded operation is considered in [13–17]. However, a single optimisation model that considers the full capabilities provided by active network management (ANM) [3], namely enabling coordinated control of network switches and DER, while considering the operation of the on-load tap changer (OLTC) for service restoration has not been proposed in previous works. In [13–17], DG units operate under a constant power factor. More specifically, control of the dispatchable DG units is not considered in [13–15], while control of renewable DG units is not considered in [16, 17]. Furthermore, in [13–17], the substation's voltage magnitude is considered fixed, and the voltage regulation provided by the OLTC is ignored. As a result, the derived service restoration plans may include unnecessary switch operations and/or additional disconnections of loads.

This paper introduces an optimisation model for the optimal service restoration of active distribution systems (ADSs). The proposed model considers the coordinated control of the available switches, DG available in the non-faulted feeders, and the operation of the OLTC to solve the service restoration problem. The proposed model consists of a single optimisation objective function aiming at minimising: (i) the out of service areas considering customer priorities, (ii) the number of switch operations, (iii) the tap changes of the OLTCs, and (iv) the active power injected through substation(s). The service restoration plan is determined considering forecasts of the load demand and renewable generation variation. Furthermore, the service restoration problem is formulated as a MISOCP problem, which uses convex relaxation of the ac power flow equations. Thus, it can be efficiently solved by a commercial branch and bound solvers, and the optimality of the solution can be guaranteed. As shown in Table 1, the proposed model is the first one that concurrently incorporates all the considered attributes of the service restoration process. Results on a 135-bus distribution system and a 540-bus distribution system are presented to demonstrate the efficiency of the proposed model.

The main contributions of this paper are

i. It proposes a service restoration model of ADSs that considers the coordinated control of network components and DG of non-faulted feeders to minimise the out of service areas with the minimum control actions.
ii. The proposed service restoration model includes the mathematical modelling of the major network components along with ANM.

2 Power flow equations and relaxations

The power flow model of the proposed service restoration model is based on the convex relaxation of the *DistFlow* equations [27]. The distribution system is assumed as balanced. Thus the equivalent single-phase network is considered. The power flow variables are illustrated in Fig. 1. The power flow equations at period t are

$$P_{ji,t} - \sum_{k \in \Omega_{\text{ch}}(i)} P_{ik,t} = P_{d,i,t} + I^{\text{sqr}}_{ji,t} \cdot r_{ij} \quad \forall i \in \Omega_N \tag{1}$$

$$Q_{ji,t} - \sum_{k \in \Omega_{\text{ch}}(i)} Q_{ik,t} = Q_{d,i,t} + I^{\text{sqr}}_{ji,t} \cdot x_{ij} \quad \forall i \in \Omega_N \tag{2}$$

$$\begin{aligned} U^{\text{sqr}}_{i,t} = U^{\text{sqr}}_{j,t} - 2 \cdot \left(r_{ij} \cdot P_{ji,t} + x_{ij} \cdot Q_{ji,t}\right) \\ +(r^2_{ij} + x^2_{ij}) \cdot I^{\text{sqr}}_{ji,t} \quad \forall ij \in \Omega_{\text{L}} \end{aligned} \tag{3}$$

$$U^{\text{sqr}}_{j,t} \cdot I^{\text{sqr}}_{ji,t} = P^2_{ji,t} + Q^2_{ji,t} \quad \forall ij \in \Omega_{\text{L}} \tag{4}$$

The active and reactive power balance equations at bus i are given by (1) and (2), respectively. The voltage drop between buses i and j is presented in (3). The squared magnitude of the current of each line is calculated by (4). The non-linear equality constraint (4) is the source of non-convexity and it is relaxed to the inequality constraint (5) [28].

$$U^{\text{sqr}}_{j,t} \cdot I^{\text{sqr}}_{ji,t} \geq P^2_{ji,t} + Q^2_{ji,t} \quad \forall ij \in \Omega_{\text{L}} \tag{5}$$

The relaxation above is exact for radial distribution networks [29, 30]. The power flow equations are

$$P_{ji,t} - \sum_{k \in \Omega_{\text{ch}}(i)} P_{ik,t} = P_{d,i,t} + PL_{i,t} \quad \forall i \in \Omega_N \tag{6}$$

$$Q_{ji,t} - \sum_{k \in \Omega_{\text{ch}}(i)} Q_{ik,t} = Q_{d,i,t} + QL_{i,t} \quad \forall i \in \Omega_N \tag{7}$$

$$U_{j,t}^{\text{sqr}} \cdot PL_{i,t} \geq r_{ij} \cdot \left(P_{ji,t}^2 + Q_{ji,t}^2\right) \quad \forall ij \in \Omega_{\text{L}} \tag{8}$$

$$U_{j,t}^{\text{sqr}} \cdot QL_{i,t} \geq x_{ij} \cdot \left(P_{ji,t}^2 + Q_{ji,t}^2\right) \quad \forall ij \in \Omega_{\text{L}} \tag{9}$$

$$U_{i,t}^{\text{sqr}} = U_{j,t}^{\text{sqr}} - 2 \cdot \left(r_{ij} \cdot P_{ji,t} + x_{ij} \cdot Q_{ji,t}\right) \quad \forall ij \in \Omega_{\text{L}} \tag{10}$$

Considering that $PL_{i,t} = I_{ji,t}^{\text{sqr}} \cdot r_{ij}$ and $QL_{i,t} = I_{ji,t}^{\text{sqr}} \cdot x_{ij}$, (1) and (2) are transformed to (6) and (7), respectively. Based on (5), the active and reactive line loss terms are calculated by (8) and (9), respectively. Constraints (6) and (7) are hyperbolic constraints, which belong to the class of second-order cone programming constraints [28]. Neglecting the last quadratic term of (3), the voltage drop between two buses is calculated by the linear equality constraint (10).

3 Problem formulation

When a fault occurs, the circuit breaker installed at the source of the feeder or a recloser automatically opens and interrupts the power supply of the feeder. After the fault is isolated, service restoration determines the appropriate control actions that result in a temporary network configuration until the cause of the outage is eliminated, i.e. repair or replacement of the faulted network component. It should be noted that the system for reconfiguration often changes. Thus, the solution to this problem requires a flexible model that allows the analysis of multiple objectives and constraints, which may vary among different distribution system operator (DSO) practices. After the service restoration plan is determined, a strategy that provides the sequence of switching actions should be followed [25, 26, 31].

It is assumed that information and communication technology and advanced metering infrastructure have been already installed in the network to enable the application of ANM that is used for network optimal operation under normal conditions [32] and not solely for the application of the proposed method. The ANM scheme employed incorporates the coordinated control of the switches, the reactive power of the available DG and the operation of OLTC for the optimal solution of the service restoration problem. Furthermore, it is considered that the load buses can be disconnected separately from the network. It should be noted that the switches are remote controlled switches. It is also considered that according to established practices, when a fault occurs in a distribution feeder, the DG units connected to this feeder are automatically disconnected. Hence, DG units are not considered capable to serve as black-start units, preventing the islanded operation of the network. However, DG units at adjacent feeders can be used to provide voltage support at the infeeding substation.

3.1 Input data

The loading conditions of the distribution system are an important factor for the computation of the optimal service restoration plan. Most works [6–11, 13–15] consider the rated load to solve the problem. However, this assumption may lead to additional switch operations or unnecessary disconnection of load buses from the network [16], if line capacity and voltage constraints are included in the formulation of the problem.

The duration that the system is at restorative state (T_{out}) is equal with the time needed to repair or replace the faulted network component. Depending on the fault cause, the repair or replacement of the faulted network component may last several hours, in which load demand and renewable generation will change. Load and renewable generation forecasts are therefore required for the estimated duration of the restorative state. It should be noted that the load forecast immediately after the power supply is restored is not straightforward. In the proposed method, it is assumed that the interrupted customers consume: (i) their rated load for the first hour immediately after their power supply is restored and (ii) their forecasted load profile for the rest of the period the system is at the restorative state. The part of the network that is not affected by the outage serves the forecasted load and renewable generation. It should be noted that load and renewable generation forecasts are frequently used for the optimal operation of ADSs under normal operating conditions [32].

3.2 Optimisation model

The proposed optimisation model adapts the convex relaxations of the ac power flow equations for radial distribution networks [27, 28]. For service restoration of ADSs, the optimisation model is formulated as follows:

Table 1 Contributions and attributes of the reviewed service restoration papers

Ref.	LS[a]	LS[b]	CP[c]	L-V[d]	DG	OLTC	ANM
[6, 7]	✓	✓	—	—	—	—	—
[8–10]	✓	✓	✓	—	—	—	—
[11]	✓	✓	—	—	—	✓	—
[12]	✓	✓	—	✓	—	—	—
[13–15]	✓	✓	✓	—	✓	—	—
[16, 17]	✓	✓	✓	✓	✓	—	—
proposed	✓	✓	✓	✓	✓	✓	✓

[a]Line switching.
[b]Load service.
[c]Customer priority.
[d]Load variation.

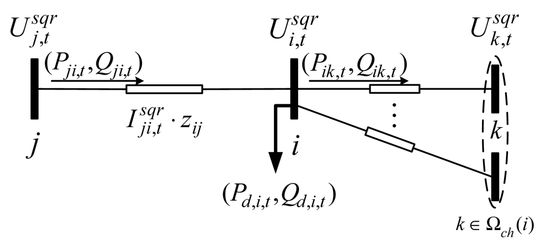

Fig. 1 *Illustration of power flow variables*

$$\min f = \sum_{k=1}^{5} f_k \tag{11}$$

where

$$f_1 = c_{\text{out}} \cdot \sum_{t \in T_{\text{out}}} \sum_{i \in \Omega_N} w_i \cdot (1 - \rho_{i,t}) \cdot P_{d,i,t} \cdot \delta_t \tag{12}$$

$$f_2 = c_{\text{sw}} \cdot \sum_{ij \in \Omega_{\text{cl}}} (1 - \text{sw}_{ij}) + c_{\text{sw}} \cdot \sum_{ij \in \Omega_{\text{op}}} \text{sw}_{ij} \tag{13}$$

$$f_3 = c_{\delta v} \cdot \sum_{t \in T_{\text{out}}} \sum_{i \in \Omega_N} \left(\delta v_{i,t}^{l} + \delta v_{i,t}^{u}\right) \tag{14}$$

$$f_4 = c_{\text{tap}} \cdot \sum_{t \in T_{\text{out}}} \sum_{i \in \Omega_{\text{OLTC}}} \left(\text{tap}_{i,t}^{+} + \text{tap}_{i,t}^{-}\right) \tag{15}$$

$$f_5 = c_{\text{ss}} \cdot \sum_{t \in \text{T}_{\text{out}}} \sum_{i \in \Omega_{\text{SS}}} P_{\text{ss},i,t} \cdot \delta_t \tag{16}$$

The objective function (11) consists of multiple objectives. The multiple objectives are transformed into a single objective function using cost-based weighting factors for each individual objective.

The first and most important objective (12) minimises the cost of the non-supplied energy, considering the priority of each load. The higher the value of the factor w_i, the higher the priority of the load. The second objective (13) represents the operation cost of the switches. By minimising the number of switch operations, the service restoration plan provides a network configuration similar to the prefault configuration, which makes simpler its implementation as well as the return to the prefault configuration after the fault clearance. A small number of switch operations also results in low operational costs and low wear of the switches. Hence, the minimisation of the number of switch operations has the second priority. Note that $\Omega_{\text{cl}} \cup \Omega_{\text{op}} = \Omega_{\text{LwS}}$. In emergency conditions, the relaxation of the voltage constraints is considered acceptable; nevertheless, they should remain within certain limits. The penalisation cost of this relaxation is given by (14). By minimising (14), the suitable tap position of the OLTC(s) and DG reactive power are derived to regulate the network bus voltages, as close as possible, within their limits. The fourth objective (15) minimises the operation cost of the OLTC. The last objective (16) can be seen as the minimisation of the cost of the energy supplied from the substation to affect least the healthy parts of the network and has the lowest priority.

The values assigned to these cost-based weighting factors depend on the importance of each objective and they should be selected according to the hierarchy of the decision variables of the service restoration problem. For example, the value of the weighting factor c_{out} should be significantly higher, at least one order of magnitude, than the weighting factor c_{sw}, so as the optimal service restoration plan will include as many switch operations as needed to avoid the disconnection of additional load buses. Similarly, the value of the weighting factor $c_{\delta v}$ should be significantly higher, at least one order of magnitude, than the weighting factor c_{tap}, so as the tap of the OLTC will be changed, only if the voltage of a bus is out of the normal operating limits. Since the last term has the lowest priority, the value of the weighting factor c_{ss} should have the lowest value. The values of the cost-based weighting factors may vary from network to network and they are determined before executing the optimisation algorithm [14, 33].

The network's operational constraints $\forall t \in T_{\text{out}}$ are as follows:

$$\begin{aligned}\sum_{j \in \Omega_N} \left(P_{ji,t} - P_{ij,t}\right) + P_{\text{ss},i,t} + P_{\text{dg},i,t} \\ = P_{d,i,t} \cdot \rho_{i,t} + PL_{i,t} \quad \forall i \in \Omega_N\end{aligned} \tag{17}$$

$$\begin{aligned}\sum_{j \in \Omega_N} \left(Q_{ji,t} - Q_{ij,t}\right) + Q_{\text{ss},i,t} + Q_{\text{dg},i,t} \\ = Q_{d,i,t} \cdot \rho_{i,t} + QL_{i,t} \quad \forall i \in \Omega_N\end{aligned} \tag{18}$$

$$\begin{aligned}r_{ij} \cdot \left(P_{ji,t}^2 + Q_{ji,t}^2\right) \le \text{Aux}U_{i,t}^{\text{sqr}} \cdot PL_{i,t} \\ \forall ij \in \Omega_{\text{L}}\end{aligned} \tag{19}$$

$$\begin{aligned}x_{ij} \cdot \left(P_{ji,t}^2 + Q_{ji,t}^2\right) \le \text{Aux}U_{i,t}^{\text{sqr}} \cdot QL_{i,t} \\ \forall ij \in \Omega_{\text{L}}\end{aligned} \tag{20}$$

$$\begin{aligned}\text{Aux}U_{i,t}^{\text{sqr}} \le U_{j,t}^{\text{sqr}} + M \cdot \left(1 - y_{ji}\right) \\ \forall ij \in \Omega_{\text{L}}\end{aligned} \tag{21}$$

$$\begin{aligned}\text{Aux}U_{i,t}^{\text{sqr}} \ge U_{j,t}^{\text{sqr}} - M \cdot \left(1 - y_{ji}\right) \\ \forall ij \in \Omega_{\text{L}}\end{aligned} \tag{22}$$

$$\begin{aligned}U_{i,t}^{\text{sqr}} \le U_{j,t}^{\text{sqr}} - 2 \cdot \left(r_{ij} \cdot P_{ji,t} + x_{ij} \cdot Q_{ji,t}\right) \\ +M \cdot \left(1 - y_{ji}\right) \quad \forall ij \in \Omega_{\text{L}}\end{aligned} \tag{23}$$

$$\begin{aligned}U_{i,t}^{\text{sqr}} \ge U_{j,t}^{\text{sqr}} - 2 \cdot \left(r_{ij} \cdot P_{ji,t} + x_{ij} \cdot Q_{ji,t}\right) - M \cdot \left(1 - y_{ji}\right) \\ \forall ij \in \Omega_{\text{L}}\end{aligned} \tag{24}$$

$$-M \cdot y_{ij} \le P_{ij,t} \le M \cdot y_{ij} \quad \forall ij \in \Omega_{\text{L}} \tag{25}$$

$$-M \cdot y_{ij} \le Q_{ij,t} \le M \cdot y_{ij} \quad \forall ij \in \Omega_{\text{L}} \tag{26}$$

$$P_{ij,t}^2 + Q_{ij,t}^2 \le S_{\text{lim},ij}^2 \quad \forall ij \in \Omega_{\text{L}} \tag{27}$$

$$P_{\text{ss},i,t}^2 + Q_{\text{ss},i,t}^2 \le S_{\text{SS},i}^2 \quad \forall ij \in \Omega_{\text{L}} \tag{28}$$

$$V_{\min}^2 - \delta v_{i,t}^{l} \le U_{i,t}^{\text{sqr}} \le V_{\max}^2 + \delta v_{i,t}^{u} \quad \forall i \in \Omega_N \tag{29}$$

$$0 \le \delta v_{i,t}^{l}, \quad \delta v_{i,t}^{u} \le \delta v^{tr} \quad \forall i \in \Omega_N \tag{30}$$

$$y_{ij} + y_{ji} = 1 \quad \forall ij \in \Omega_{\text{L}} \setminus \Omega_{\text{LwS}} \tag{31}$$

$$y_{ij} + y_{ji} = \text{sw}_{ij} \quad \forall ij \in \Omega_{\text{LwS}} \tag{32}$$

$$\sum_{j \in \Omega_N} y_{ji} = 1 \quad \forall i \in \Omega_N \setminus \Omega_{\text{SS}} \tag{33}$$

$$y_{ji} = 0 \quad \forall i \in \Omega_{\text{SS}} \tag{34}$$

The active and reactive power balance at each node during the restorative state is represented by (17) and (18), respectively. A distribution network can be considered as a spanning tree, if it has one substation [34] or as a spanning forest if it has more. Thus, a bus can have only one parent except for the root of the tree, which is the substation(s). If bus j is the parent of bus i ($y_{ji} = 1$), the combination of (19), (21) and (22) yields the active power loss on the line that connects these two buses, as presented in (8). Otherwise, if buses i and j are not connected, constraints (19), (21) and (22) become inactive, since M takes a large value. A strategy for selecting reasonable values for M is presented in [35]. Similarly, the reactive power loss on each line at period t is calculated by (20)–(22). The voltage drop between buses i and j at period t is calculated by (23) and (24), in case buses i and j are connected. According to (25) and (26), the active and reactive powers flow on each line at period t are equal to zero, respectively, when buses i and j are not connected. The capacity limits of each line and substation are given by (27) and (28), respectively. The relaxed voltage magnitude limits at period t are given by (29). As shown in (30), the variables $\delta v_{i,t}^{l}$ and $\delta v_{i,t}^{u}$ are greater than or equal to zero and the voltage limits can be relaxed to a certain value. The radiality of the restored network topology is ensured by (31)–(34).

If lines i–j are part of the spanning tree ($\text{sw}_{ij} = \text{sw}_{ji} = 1$), bus i will be the parent of bus j ($y_{ij} = 1$) or bus j will be the parent of bus i ($y_{ji} = 1$), as shown in (31) and (32). Equation (33) ensures that each bus can have only one parent, while (34) guarantees that the substation has no parents.

The voltage on the MV bus of the substation transformer can be regulated to the desired value by the installed OLTC at the HV/MV substation. The tap position of the OLTC takes integer values. It determines the substation's voltage $\forall t \in T_{\text{out}}$ and is modelled as follows:

$$V_{i,t} = V_{\min,i} + \text{tap}_{i,t} \cdot \text{Step}_{\text{OLTC}} \quad \forall i \in \Omega_{\text{OLTC}} \tag{35}$$

$$U_{i,t}^{\text{sqr}} = (1 + \text{tap}_{i,t} \cdot \text{Step}_{\text{OLTC}})^2 \quad \forall i \in \Omega_{\text{OLTC}} \tag{36}$$

$$U_{i,t}^{\text{sqr}} = 1 + 2 \cdot \text{tap}_{i,t} \cdot \text{Step}_{\text{OLTC}} \quad \forall i \in \Omega_{\text{OLTC}} \tag{37}$$

$$\text{tap}_{i,t+1} - \text{tap}_{i,t} = \text{tap}_{i,t}^{+} - \text{tap}_{i,t}^{-} \quad \forall i \in \Omega_{\text{OLTC}} \tag{38}$$

$$\text{tap}_{i,t}^{-}, \text{tap}_{i,t}^{+} \geq 0 \quad \forall i \in \Omega_{\text{OLTC}} \tag{39}$$

$$\text{tap}_{i,t} \leq \text{tap}_{\max} \quad \forall i \in \Omega_{\text{OLTC}} \tag{40}$$

It is assumed that the minimum voltage of the substation is equal to 1.0 p.u. in (35). The quadratic constraint (36) is linearised to (37) using the binomial approximation. The binomial approximation states that if $|x| < 1$ and $|ax| \ll 1$, then $(1 + x)^a \ll 1 + ax$. Thus, it can be applied to (36), since the step voltage of the OLTC takes small values, e.g. 0.625% of the rated voltage. The number of the tap position changes is given by (38). It should be noted that the variables $\text{tap}_{i,t}^{-}$ and $\text{tap}_{i,t}^{+}$ are greater than or equal to zero (39) and their sum is minimised (15). The minimisation of (15) has, as a result, one of the two variables $(\text{tap}_{i,t}^{-}, \text{tap}_{i,t}^{+})$ to be equal to zero, while the other one determines the number of the tap position changes. The range limit of the tap position is presented in (40).

In the proposed service restoration method, the control of the reactive power of the DG units is considered. More specifically, the DG units are enabled to absorb or supply reactive power, as shown in Fig. 2 and it is formulated $\forall t \in T_{\text{out}}$ as follows:

$$\text{If} \quad 0 \leq P_{\text{dg},i,t} \leq 0.05 \cdot P_{\text{DG},i}^{\text{rated}}: \quad Q_{\text{dg},i,t} = 0 \tag{41}$$

$$\begin{gathered}\text{If} \quad 0.05 \cdot P_{\text{DG},i}^{\text{rated}} \leq P_{\text{dg},i,t} \leq 0.2 \cdot P_{\text{DG},i}^{\text{rated}}: \\ -2.42 \cdot P_{\text{dg},i,t} \leq Q_{\text{dg},i,t} \leq 2.42 \cdot P_{\text{dg},i,t}\end{gathered} \tag{42}$$

$$\begin{gathered}\text{If} \quad 0.2 \cdot P_{\text{DG},i}^{\text{rated}} \leq P_{\text{dg},i,t} \leq P_{\text{DG},i}^{\text{rated}}: \\ -0.484 \cdot P_{\text{DG},i}^{\text{rated}} \leq Q_{\text{dg},i,t} \leq 0.484 \cdot P_{\text{DG},i}^{\text{rated}}\end{gathered} \tag{43}$$

$$P_{\text{dg},i,t}^2 + Q_{\text{dg},i,t}^2 \leq (S_{\text{DG},i}^{\text{rated}})^2 \tag{44}$$

The reactive power supplied or absorbed by the DG units is limited by the fixed apparent power capacity of their inverter, as shown in (44). It should be noted that the inverters are oversized compared to the rated active power of the DG units.

The proposed service restoration model aims at minimising (11) subject to (17)–(34) and (37)–(44). The proposed optimisation model is MISOCP due to the second-order cone constraints (19) and (20). The proposed optimisation model is implemented in GAMS [36], and it is solved using the commercial CPLEX solver [37].

4 Results and discussion

The proposed service restoration method is tested using the modified 135-bus distribution system [37], presented in Fig. 3. This system is a 13.8 kV network, with two substations (S/S), 8 feeders, 105 load buses, 8 circuit breakers (CBs), 29 NC switches and 21 NO switches. The detailed data of the network can be found in Appendix. Five solar DG units of 500 kW are connected at buses 94–96, 102, and 120; seven solar DG units of 1 MW are connected at buses 90–93, 97, 98, and 107; two wind DG units of 5 and 2 MW are connected at bus 15 and bus 82, respectively. The total rated power of solar and wind DG units are 23.75 and 17% of the total rated load, respectively. Fig. 4 presents the day-ahead forecasted hourly profile of load demand, solar generation and wind generation. The capacity of each substation is 25 MVA and they are both equipped with OLTCs. The step voltage of the OLTCs is equal to 0.625% of the nominal voltage. The thermal capacity of each line is 10 MVA. The voltage limits at normal operating conditions are considered equal to ±5% of the nominal voltage; while at emergency conditions, they are equal to ±10% of the nominal voltage. The load buses 10–16, 51–61, 24–30, and 121–135 have the highest priority and their w_i is equal to 10, while for the rest buses w_i are equal to 1. The values of the weighting factors are $c_{\text{out}} = 10$, $c_{\text{sw}} = 1$, $c_{\delta v} = 1$, $c_{\text{tap}} = 0.1$ and $c_{\text{ss}} = 0.01$. The values of the weighting factors are selected according to the preferred options described in Section 3.2 and small variations of these weighting factors do not affect the results. The value of parameter M is equal to 10. All tests were performed on a PC with an Intel Core i7 CPU at 3.40 GHz and 4 GB of RAM.

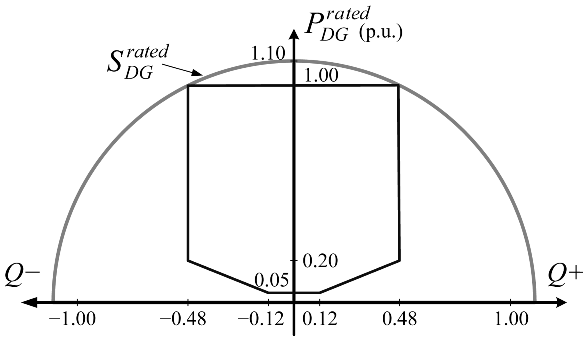

Fig. 2 *Reactive power capability curve of DG units*

Three cases are analysed to examine the effect of the ANM and renewable DG on the solution of the service restoration problem. The three cases are as follows:

- *Case I:* The service restoration plan is determined based only on rated load, while DG is not considered. The substations' voltages are fixed at their prefault values, i.e. the operation of the OLTC is not considered. The optimisation model is given by (11)–(13) and (17)–(34).
- *Case II:* The service restoration plan is determined based only on rated load, while DG is not considered. The operation of the OLTC is considered. The optimisation model is given by (11)–(34) and (37)–(40).
- *Case III:* The service restoration plan is determined considering the load and renewable DG variation, as described in Section 3.1 and exploiting the ANM control capabilities. The optimisation model is given by (11)–(34) and (37)–(44).

It should be noted that in Case I, the service restoration problem is solved based on the same assumptions as in [8–10], while in Case III, the proposed model is solved.

4.1 Results of the 135-bus distribution system: fault on line 39-40

It is assumed that a fault on line 39-40 occurs between 10:00 and 11:00. The prefault voltage of the substation buses 201 and 202 is 1.025 p.u. The CB installed on line 201-39 is tripped and the power supply of load buses 39–62 is interrupted. After identifying the fault location, the NC switch installed on line 40–42 is opened and the faulted area is isolated. Buses 39–41 will be out of service until the fault is cleared. The duration of the restorative state is estimated at 5 h. Service restoration aims at restoring the power supply of the non-faulted area, i.e. buses 42–62.

i. *Case I:* The service restoration plan requires the disconnection of buses 46 and 105 from the restored network to maintain their operating limits at emergency conditions. Furthermore, three switch operations are required to determine the restored network topology, i.e. the NC switch on line 47-48 is opened, while the NO switches on lines 25–51 and 62–120 are closed. The voltage magnitude for eight buses is below 0.92 p.u., with a minimum voltage of 0.915 p.u. at bus 61. The total computation time of the optimisation model is 2.75 min.

ii. *Case II:* The service restoration plan does not require the disconnection of additional load buses, while the operation of three switches is needed, i.e. the NC switch on line 47-48 is opened and the NO switches on lines 55–98 and 62–120 are closed. The voltage magnitude of bus 201 keeps its prefault value, while the voltage magnitude of bus 202 is equal to 1.10 p.u. In this case, the calculated tap changes of the OLTC at S/S 2 are equal to 12. The voltage magnitude for ten buses is below 0.94 p.u., with a minimum voltage of 0.927 p.u. at bus 44. The total computation time of the optimisation model is 0.85 min.

iii. *Case III:* The restored network topology is illustrated in Fig. 5, where the faulted and isolated area is included within a box filled with a dark grey background, while the restored area within a box filled with a light grey background. The service restoration plan of the proposed method does not require the disconnection of additional loads. Furthermore, only one switch operation, i.e. closing of the switch on line 55–98, is required. The non-supplied buses 42–62 are transferred to feeder F7, which accommodates a considerable amount of solar DG. The voltage magnitude at substation bus 202 is 1.0625 p.u. during the restorative state. Hence, the tap changes of the OLTC at S/S 2 are 6. The reactive power support provided by the DG units of F7 along with the operation of the OLTC facilitate the operation of the restored network closer to its normal operating limits. The minimum voltage of the network is 0.948 p.u. at bus 44 from 11:00–12:00. The total computation time of the optimisation model is 1.21 min.

A summary comparison of the service restoration plans of Cases I–III is presented in Table 2. Furthermore, Fig. 6 shows the voltage profile of the restored buses, i.e. buses 42–62, in Cases I and III, during the first hour after the power supply is restored. It can be seen that the service restoration plan of the proposed method, which exploits the reactive power capability of the available DG units and the operation of the OLTC, requires significant less control action, i.e. only one switch operation, and ensures the operation of the restored network closer to its normal operating limits.

4.2 Results of the 135-bus distribution system: fault on line 18-19

In this section, a fault on line 18-19 between 17:00 and 18:00 is simulated. The prefault voltage of the substation buses 201 and 202 is 1.025 and 1.0375 p.u., respectively. Initially, the CB on line 201-17 is tripped interrupting the power supply of buses 17–38. The fault is identified next and the switch on line 19-20 is opened to isolate the faulted area. The power supply of buses 17–19 is not restored until the outage cause is cleared. The duration of the restorative state is estimated at 5 h. The objective of the service restoration is to restore the power supply of the non-faulted area, i.e. buses 20–38.

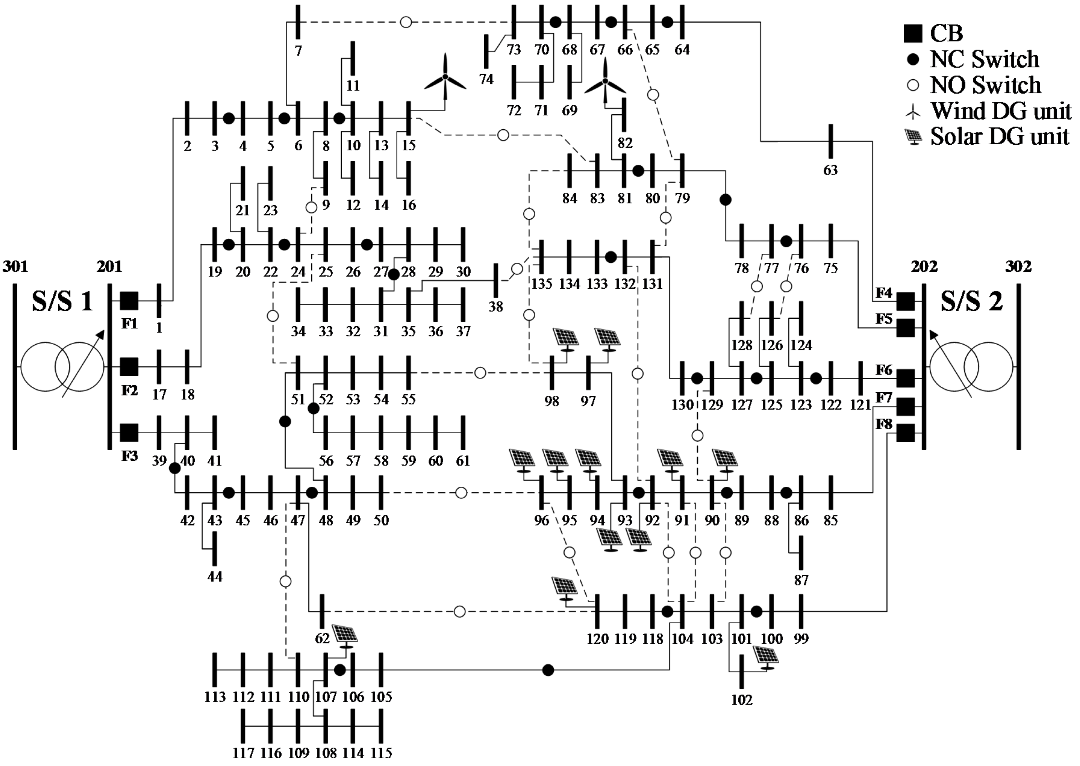

Fig. 3 *Modified 135-bus distribution system*

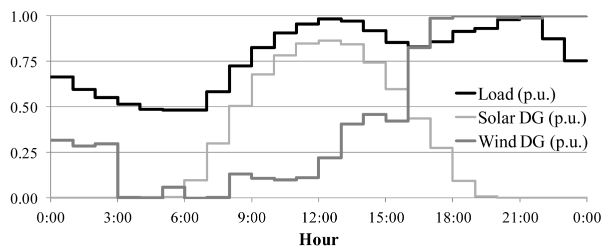

Fig. 4 *Forecasted hourly profile of load demand, solar generation and wind generation*

i. *Case I:* The restored network topology is obtained by disconnecting the load buses 34 and 46 and by operating three switches. The switch on line 28–31 is opened and the switches on lines 25–51 and 38–135 are closed. As a result, the load demand of buses 20–30 is transferred to feeder F1, while the load demand of buses 34–38 is transferred to feeder F6. The voltage for ten buses is below 0.92 p.u., with a minimum voltage of 0.910 p.u. at bus 37. The computation time is 3.49 min.

ii. *Case II:* The service restoration plan does not require the disconnection of additional load buses and the operation of three switches is needed, i.e. the NC switch on line 8–10 is opened and the NO switches on lines 9–24 and 15–83 are closed. The voltage magnitude of bus 201 is equal to 1.09375 p.u., while the voltage magnitude of bus 202 is equal to 1.10 p.u. In this case, the tap changes of the OLTCs at S/S 1 and at S/S 2 are equal to 11 and 10, respectively. The voltage magnitude for 11 buses is below 0.95 p.u., with a minimum voltage of 0.920 p.u. at bus 12. The total computation time is 0.64 min.

iii. *Case III:* The service restoration plan does not require the disconnection of additional load buses and the operation of one switch is needed. More specifically, the NO switch on line 9–24 is closed and the healthy part of the feeder F2 is entirely transferred to feeder F1, which accommodates a significant amount of wind DG. As a result of this load transfer, the voltage of the substation bus 201 needs to change from its prefault value, i.e. 1.025 p.u., to 1.075 p.u. and the wind DG

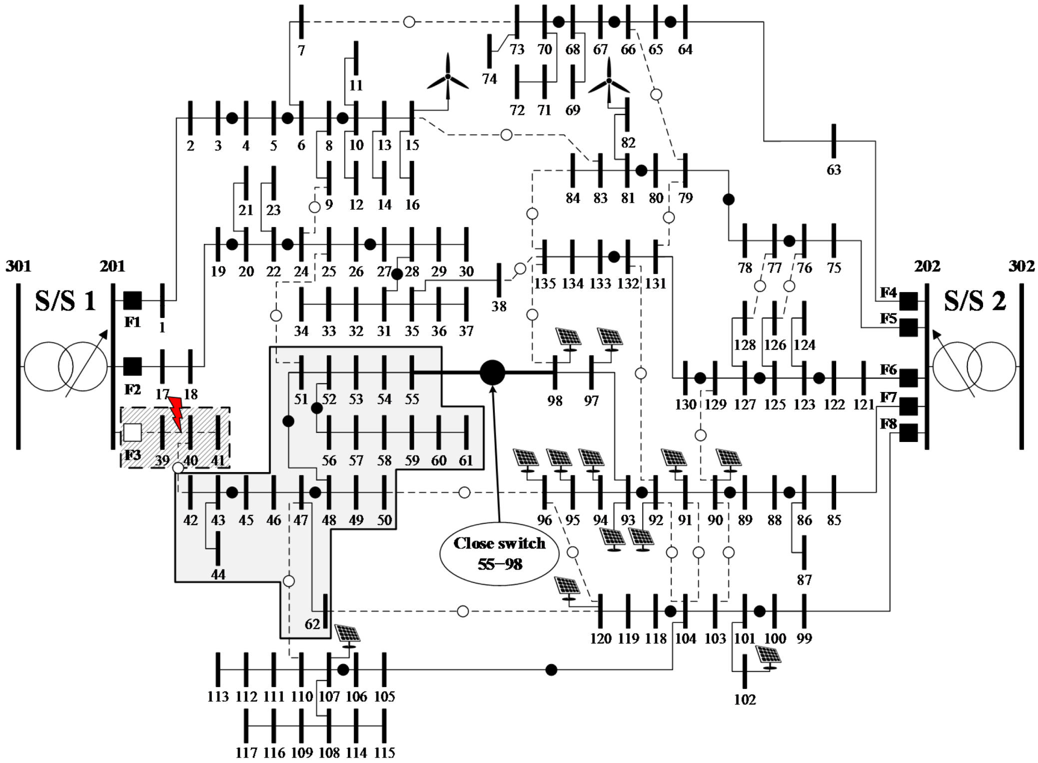

Fig. 5 *Restored network topology of the modified 135-bus distribution system due to fault on line 39-40 in Case II*

Table 2 Summary comparison of the service restoration plans of the 135-bus distribution system in Cases I–III considering a fault on line 39-40

	Case I	Case II	Case III
disconnection of additional load buses	Bus 46	none	none
	Bus 105		
number of switch operations	3	3	1
V_{201}, p.u.	1.025	1.025	1.025
V_{202}, p.u.	1.025	1.10	1.0625
minimum voltage magnitude	0.915 p.u. at bus 61	0.927 p.u. at bus 44	0.948 p.u. at bus 44 (11:00–12:00)
computation time, min	2.75	0.85	1.21

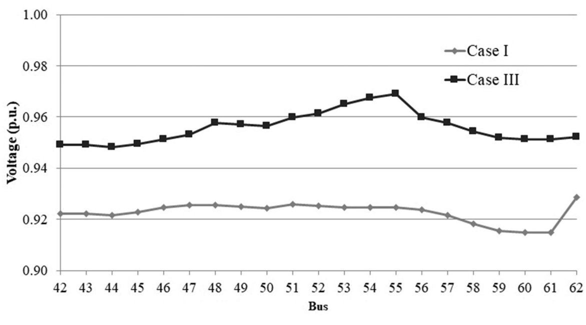

Fig. 6 *Voltage profile of the restored buses of the modified 135-bus distribution system due to fault on line 39-40 in Cases I and III*

unit at bus 15 is enabled to supply reactive power in order to facilitate the operation of the network close to its normal operating limits. Therefore, in this case, the total tap changes are equal to 8 and the minimum voltage magnitude of the network is 0.940 p.u. at bus 37 during 21:00–22:00. The voltage of substation bus 202 is equal to its prefault value, i.e., 1.0375 p.u. The total computation time is 1.74 min.

A summary comparison of the results of Cases I–III is shown in Table 3. Fig. 7 shows the voltage profile of the restored buses, i.e. buses 20–38, in Cases I and III, during the first hour after the power supply is restored. By comparing the results of Cases I–III, it is shown that to determine a service restoration plan with the minimum control actions and the minimum out of service area, it is necessary to consider the operation of the OLTC, the available DG and the reactive power capabilities of the DG units.

Table 3 Summary comparison of the service restoration plans of the 135-bus distribution system in Cases I–III considering a fault on line 18-19

	Case I	Case II	Case III
disconnection of additional load buses	Bus 34 Bus 46	none	none
number of switch operations	3	3	1
V_{201}, p.u.	1.025	1.09375	1.075
V_{202}, p.u.	1.0375	1.10	1.0375
minimum voltage magnitude	0.910 p.u. at bus 37	0.920 p.u. at bus 12	0.940 p.u. at bus 37 (21:00–22:00)
computation time, min	3.49	0.64	1.74

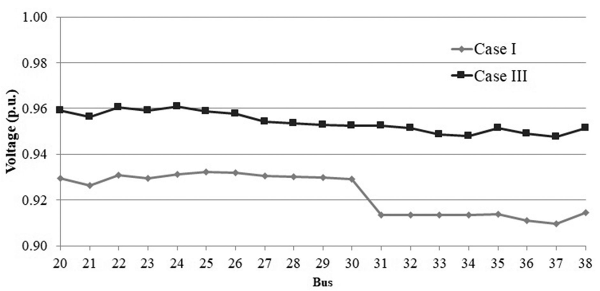

Fig. 7 *Voltage profile of the restored buses of the modified 135-bus distribution system due to fault on line 18-19 in Cases I and III*

4.3 Results of the 135-bus distribution system: additional simulations

Apart from the fault cases presented in Sections 4.1 and 4.2, additional simulations are run to provide statistically summarised results of the proposed model (Case III) compared with the models of Cases I and II. More specifically, the maximum number of different single fault occasions that can be simulated is 28. These 28 different single fault occasions are simulated for Cases I–III. Table 4 presents a summary comparison of the results of the additional simulations for Cases I–III. As shown in Table 4, Case I needs the lowest computation time, since the optimisation model of this case is the least complex. However, the derived service restoration plans of Case I require sometimes the disconnection of additional load buses and the operation of more switches compared with Cases II and III. More specifically, in Case I, the disconnection of additional buses is required in 4 out of 28 fault cases, while the service restoration plans derived by the proposed model do not require the disconnection of any additional buses in any fault case. Furthermore, in Case I, in 7 out of the 28 fault cases, the service restoration plans require 3 switch operations, while the service restoration plans derived by the proposed model require only one switch operation in all fault cases. By comparing the results of Cases II and III, it is shown that in order to determine a service restoration plan with the minimum switch operations, the consideration of the OLTC operation is not enough. It is also necessary to consider the available DG units and their capability to provide reactive power support.

4.4 Results of the 135-bus distribution system: multiple faults

To further analyse the performance of the proposed service restoration method, multiple faults are simulated. More specifically, it is assumed that two faults occur simultaneously on lines 20-22 and 39-40 between 10:00 and 11:00. The prefault voltage of the substation buses 201 and 202 is 1.025 p.u. The CBs on lines 201-17 and 201-39 are tripped and the power supply of feeders F2 and F3 is interrupted. After identifying the fault locations, the NC switches on lines 19-20, 22–24 and 40–42 are opened and the two faulted areas are isolated. The buses 20–23 and 39–41 are out of service until the cause of the outage is cleared. It is assumed that the duration of the restorative state is 5 h. After the fault isolation, the CB on line 201-17 is closed. Service restoration aims at defining the appropriate control actions to restore the power supply of the non-faulted area, i.e., buses 24–38 and 42–62.

The service restoration plan is determined by the proposed method (Case III). The service restoration plan does not require the disconnection of additional load buses, but only the operation of four switches, namely, the NC switch on line 28–31 is opened and the NO switches on lines 9–24, 38–135 and 55–98 are closed. The

Table 4 Summary comparison of the service restoration plans of the 135-bus distribution system in Cases I–III considering single fault

	Min	Average	Max	SD[a]
Case I				
number of additional disconnected load buses	0	0.21	2	0.57
number of switch operations	1	1.50	3	0.88
minimum voltage magnitude, p.u.	0.910	0.933	0.951	0.016
computation time, min	0.21	0.66	3.49	0.78
Case II				
number of additional disconnected load buses	0	0	0	—
number of switch operations	1	1.29	3	0.71
minimum voltage magnitude, p.u.	0.920	0.943	0.956	0.013
computation time, min	0.61	0.73	0.85	0.07
Case III				
number of additional disconnected load buses	0	0	0	—
number of switch operations	1	1	1	—
minimum voltage magnitude, p.u.	0.940	0.956	0.961	0.010
computation time, min	0.94	1.44	1.74	0.21

[a]SD stands for standard deviation.

Table 5 Weighting factors in different scenarios

Scenario	Weighting factors				
	c_{out}	c_{sw}	$c_{\delta v}$	c_{tap}	c_{ss}
A	10	1	1	0.1	0.01
B	50	5	5	0.5	0.05
C	100	10	10	1	0. 1
D	500	50	50	5	0. 5
E	1000	100	100	10	1

Table 6 Result comparison between the proposed model and the model of [14] for a fault on zone 7 of the 44-bus distribution test system

	Model of [14]	Proposed model
Without DG and with load shedding capability		
load shedding	34.8% of the load at bus 43	35.2% of the load at bus 43
switch operations	open: 22–25	open: 22–25
	close: 12–28, 23–39	close: 12–28, 23–39
minimum voltage magnitude	0.950 p.u. at bus 44	0.950 p.u. at bus 44
With DG and without load shedding capability		
load shedding, %	0	0
switch operations	open: 22–25	open: 22–25
	close: 12–28, 23–39	close: 12–28, 23–39
minimum voltage magnitude	0.952 p.u. at bus 30	0.952 p.u. at bus 30

voltage magnitude at substation bus 201 and bus 202 is 1.05 and 1.075 p.u., respectively, during the restorative state. Therefore, the tap changes of the OLTCs at S/S 1 and at S/S 2 are equal to 4 and 8, respectively. Furthermore, the DG units of feeders F1 and F7 provide reactive power support to the network during this period. The minimum voltage is 0.936 p.u. at bus 34 during 11:00–12:00. The total computation time is 3.35 min.

The study case of this section is also solved considering different weighting factors assigned to the terms of the objective function (11) as presented in Table 5. For all the different sets of weighting factors of Table 5, the derived service restoration plans are the same.

4.5 Results of the 540-bus distribution system

To demonstrate the applicability of the method to larger distribution networks, a 540-bus distribution system is obtained by replicating four times the modified 135-bus distribution system of Fig. 3. The layout of the 540-bus distribution system is obtained by replicating four times the layout of the 135-bus distribution system of Fig. 3, taking into account that in the 540-bus system, the four different replicas of the 135-bus system are not connected each other. Due to space limitations, the layout of the 540-bus distribution system is not shown. As can be seen in Fig. 3, the 135-bus distribution system has 8 feeders with a CB installed at their source, 29 NC switches, 21 NO switches, 12 solar DG units and 2 wind DG units. Consequently, since the 540-bus system contains four times the components of the 135-bus system, the 540-bus distribution system has 32 feeders with a CB installed at their source, 116 NC switches, 82 NO switches, 48 solar DG units and 8 wind DG units. The technical characteristics of the network components are the same with the modified 135-bus distribution system.

A single fault on line 42-43 between 09:00 and 10:00 is simulated. After the fault location and isolation, the service restoration method that incorporates the ANM determines the appropriate control actions to restore power supply to the non-faulted area of the network during the whole outage period, i.e. 5 h. The restored network configuration is obtained by closing one NO switch. No additional buses are disconnected and the total number of tap changes during the outage period is 5. The restored network topology operates within normal limits and the minimum voltage is 0.953 p.u. during the restorative state. The computation time of the optimisation model is 8.88 min.

4.6 Comparison with published results

To validate the effectiveness and accuracy of the proposed model, the results of the proposed optimisation model are compared with the results of the optimisation model for service restoration of [14]. It should be noted that the proposed service restoration model includes additional features that are not formulated in the optimisation model of [14]. Thus, the proposed model is modified in order to be comparable with the optimisation model of [14]. The proposed model minimises (12) and (13) subject to (17)–(34). Furthermore, the variable $\rho_{i,t}$ is considered as a continuous variable and its lower and upper bound are 0 and 1, respectively.

The result comparison is performed for the study case of the 44-bus distribution test system of [14] considering a fault in zone 7 and two cases are analysed. In the first case, DG is not considered and the load shedding capability is enabled, while in the second case, DG is considered and the load shedding capability is not enabled. The voltage limits and line ampacity limits of [14] are considered. Table 6 presents a summary comparison of the service restoration plans of the proposed optimisation model and the model of [14]. As shown in Table 6, the results of both optimisation models are almost identical validating the accuracy of the proposed optimisation model.

5 Conclusion

This paper proposes an optimisation model for the service restoration of ADSs. After the location and isolation of a fault, the proposed service restoration method aims at minimising the out of service areas with the minimum control actions considering the variations of load demand and renewable generation. The coordinated control of the available switches, DG reactive power and the operation of the OLTC are considered to determine the optimal service restoration plan subject to the network's operational constraints. The proposed optimisation model is formulated as a MISOCP problem and is solved by commercial branch and bound solvers in very low computation time.

Results on a 135-bus distribution system and a 540-bus distribution system are presented to demonstrate its effectiveness in two different cases. Results show that incorporating ANM and taking into account renewable DG into the service restoration plan leads to solutions with fewer control actions and disconnection of fewer loads. A strategy that determines the sequence of control actions and accurate modelling of the load behaviour of interrupted customers, after their power supply is restored, are proposed as future work.

6 Acknowledgment

This research has been co-financed by the European Union and Greek national funds through the Operational Program Competitiveness, Entrepreneurship and Innovation, under the call RESEARCH–CREATE–INNOVATE (project code: T1EDK-00450).

7 References

[1] Northcote-Green, J., Wilson, R.: '*Control and automation of electrical power distribution systems*' (Taylor & Francis, Boca Raton, FL, USA, 2007, 1st edn.)

[2] Wang, P., Li, W.: 'Reliability evaluation of distribution systems considering optimal restoration sequence and variable restoration times', *IET Gener. Transm. Distrib.*, 2007, **1**, (2), pp. 688–695

[3] Peças Lopes, J.A., Hatziargyriou, N., Mutale, J., *et al.*: 'Integrating distributed generation into electric power systems: a review of drivers, challenges and opportunities', *Elect. Power Syst. Res.*, 2007, **77**, (9), pp. 1189–1203

[4] Ćurčić, S., Özveren, C.S., Crowe, L., *et al.*: 'Electric power distribution network restoration: a survey of papers and a review of the restoration problem', *Elect. Power Syst. Res.*, 1995, **35**, (2), pp. 73–86

[5] Zidan, A., Khairalla, M., Abdrabou, A.M., *et al.*: 'Fault detection, isolation, and service restoration in distribution systems: state-of-the-art and future trends', *IEEE Trans. Smart Grid*, 2017, **8**, (5), pp. 2170–2185

[6] Sanches, D.S., London, J.B.A.Jr., Delbem, A.C.B.: 'Multiobjective evolutionary algorithm for single and multiple fault service restoration in large-scale distribution systems', *Elect. Power Syst. Res.*, 2014, **110**, pp. 144–153

[7] Luan, W.P., Irving, M.R., Daniel, J.S.: 'Genetic algorithm for supply restoration and optimal load shedding in power system distribution networks', *IEE Proc. Gener. Transm. Distrib.*, 2002, **149**, (2), pp. 145–151

[8] Pérez, R., Heydt, G., Jack, N., *et al.*: 'Optimal restoration of distribution systems using dynamic programming', *IEEE Trans. Power Deliv.*, 2008, **23**, (3), pp. 1589–1596

[9] Kleinberg, M.R., Miu, K., Chiang, H.D., *et al.*: 'Improving service restoration of power distribution systems through load curtailment of in-service customers', *IEEE Trans. Power Syst.*, 2011, **26**, (3), pp. 1110–1117

[10] Romero, R., Franco, J.F., Leão, F.B., *et al.*: 'A new mathematical model for the restoration problem in balanced radial distribution systems', *IEEE Trans. Power Syst.*, 2016, **31**, (2), pp. 1259–1268

[11] Koutsoukis, N.C., Karafotis, P.A., Georgilakis, P.S., *et al.*: 'Optimal service restoration of power distribution networks considering voltage regulation'. IEEE Manchester PowerTech, Manchester, UK, July 2017, pp. 1–6

[12] Tsai, M.-S.: 'Development of an object-oriented service restoration expert system with load variations', *IEEE Trans. Power Syst.*, 2008, **23**, (1), pp. 219–225

[13] Zidan, A., El-Saadany, E.F.: 'Service restoration in balanced and unbalanced distribution systems with high DG penetration'. IEEE Power Energy Society General Meeting, Detroit, MI, USA, July 2011, pp. 1–8

[14] Cavalcante, P.L., Lopez, J.C., Franco, J.F., *et al.*: 'Centralised self-healing scheme for electrical distribution systems', *IEEE Trans. Smart Grid*, 2016, **7**, (1), pp. 145–155

[15] Abel Hafez, A., Omran, W.A., Higazi, Y.G.: 'A decentralised technique for autonomous service restoration in active radial distribution networks', *IEEE Trans. Smart Grid*, 2018, **9**, (3), pp. 1911–1919

[16] Zidan, A., El-Saadany, E.F.: 'Incorporating load variation and variable wind generation in service restoration plans for distribution systems', *Energy*, 2013, **57**, pp. 682–691

[17] Zidan, A., El-Saadany, E.F.: 'A cooperative multiagent framework for self-healing mechanisms in distribution systems', *IEEE Trans. Smart Grid*, 2012, **3**, (3), pp. 1525–1539

[18] Pham, T.T.H., Besanger, Y., Hadjsaid, N.: 'New challenges in power system restoration with large scale of dispersed generation insertion', *IEEE Trans. Power Syst.*, 2009, **24**, (1), pp. 398–406

[19] Nguyen, C.P., Flueck, A.J.: 'Agent based restoration with distributed energy storage support in smart grids', *IEEE Trans. Smart Grid*, 2012, **3**, (2), pp. 1029–1038

[20] Song, I., Jung, W.W., Kim, J.Y., *et al.*: 'Operation schemes of smart distribution networks with distributed energy resources for loss reduction and service restoration', *IEEE Trans. Smart Grid*, 2013, **4**, (1), pp. 367–374

[21] De Quevedo, P.M., Contreras, J., Rider, M.J., *et al.*: 'Contingency assessment and network reconfiguration in distribution grids including wind power and energy storage', *IEEE Trans. Sustain. Energy*, 2015, **6**, (4), pp. 1524–1533

[22] Chen, C., Wang, J., Qiu, F., *et al.*: 'Resilient distribution system by microgrids formation after natural disasters', *IEEE Trans. Smart Grid*, 2016, **7**, (2), pp. 958–966

[23] Wang, Z., Wang, J.: 'Self-healing resilient distribution systems based on sectionalisation into microgrids', *IEEE Trans. Power Syst.*, 2015, **30**, (6), pp. 3139–3149

[24] Wang, Z., Wang, J.: 'Service restoration based on AMI and networked MGs under extreme weather events', *IET Gener. Transm. Distrib.*, 2017, **11**, (2), pp. 401–408

[25] Chen, B., Chen, C., Wang, J., *et al.*: 'Multi-time step service restoration for advanced distribution systems and microgrids', *IEEE Trans. Smart Grid*, 2017, **9**, (6), pp. 6793–6805

[26] Chen, B., Chen, C., Wang, J., *et al.*: 'Sequential service restoration for unbalanced distribution systems and microgrids', *IEEE Trans. Power Syst.*, 2018, **33**, (2), pp. 1507–1520

[27] Baran, M., Wu, F.: 'Network reconfiguration in distribution systems for loss reduction and load balancing', *IEEE Trans. Power Deliv.*, 1989, **4**, (2), pp. 1401–1407

[28] Taylor, J.A., Hover, F.S.: 'Convex models of distribution system reconfiguration', *IEEE Trans. Power Syst.*, 2012, **27**, (3), pp. 1407–1413

[29] Farivar, M., Low, S.H.: 'Branch flow model: relaxations and convexification – part I', *IEEE Trans. Power Syst.*, 2013, **28**, (3), pp. 2554–2564

[30] Farivar, M., Low, S.H.: 'Branch flow model: relaxations and convexification – part II', *IEEE Trans. Power Syst.*, 2013, **28**, (3), pp. 2565–2572

[31] Marques, L.T., Delbem, A.C.B., London, J.B.A.Jr.: 'Service restoration with prioritization of customers and switches and determination of switching sequence', *IEEE Trans. Smart Grid*, 2018, **9**, (3), pp. 2359–2370

[32] Evangelopoulos, V.A., Georgilakis, P.S., Hatziargyriou, N.D.: 'Optimal operation of smart distribution networks: a review of models, methods and future research', *Elect. Power Syst. Res.*, 2016, **140**, pp. 95–106

[33] López, J.C., Franco, J.F., Rider, M.J., *et al.*: 'Optimal restoration/maintenance switching sequence of unbalanced three-phase distribution systems', *IEEE Trans. Smart Grid*, 2018, **9**, (6), pp. 6058–6068

[34] Jabr, R.A., Singh, R., Pal, B.C.: 'Minimum loss network reconfiguration using mixed-integer convex programming', *IEEE Trans. Power Syst.*, 2012, **27**, (2), pp. 1106–1115

[35] Hijazi, H., Thiébaux, S.: 'Optimal distribution systems reconfiguration for radial and meshed grids', *Int. J. Electr. Power Energy Syst.*, 2015, **72**, pp. 136–143

[36] McCarl, B.A.: 'GAMS user guide, version 23.8', 2012. Available at http://www.gams.com

[37] IBM. IBM ILOG CPLEX. Available at: http://www01.ibm.com/software/integration/optimisation/cplex-optimiser/

[38] Guimaraes, M., Castro, C.: 'Reconfiguration of distribution systems for loss reduction using tabu search'. 15th Power Systems Computation. Conf., Liège, Belgium, August 2005, pp. 1–6

6 Appendix

The detailed line data of the 135-bus distribution system can be found in [38] and the bus load data are shown in Table 7.

Table 7 Load data of the modified 135-bus distribution system

Bus *i*	$P_{d.i}$, MW	$Q_{d.i}$, Mvar	Bus *i*	$P_{d.i}$, MW	$Q_{d.i}$, Mvar	Bus *i*	$P_{d.i}$, MW	$Q_{d.i}$, Mvar
2	0.119	0.048	48	0.589	0.250	91	0.119	0.051
3	0.106	0.042	50	0.273	0.116	92	0.131	0.056
4	0.218	0.087	52	0.182	0.077	94	0.111	0.047
5	0.778	0.310	53	0.646	0.274	95	0.348	0.148
6	0.372	0.148	54	0.173	0.073	96	0.213	0.090
7	0.597	0.237	55	0.055	0.023	98	0.115	0.049
8	0.156	0.062	57	0.051	0.022	100	0.062	0.026
9	0.311	0.124	58	0.376	0.160	101	0.072	0.030
10	0.350	0.139	59	0.552	0.234	102	0.011	0.005
11	0.292	0.116	60	0.231	0.098	104	0.301	0.128
12	0.623	0.248	62	0.567	0.240	105	1.808	0.766
13	0.729	0.290	64	0.882	0.351	106	0.376	0.159
14	0.759	0.302	65	0.249	0.099	107	0.096	0.041
15	0.538	0.214	66	0.249	0.099	108	0.062	0.026
16	0.496	0.198	67	0.311	0.124	110	0.243	0.103
20	0.075	0.037	68	0.529	0.211	111	0.073	0.031
21	0.577	0.282	69	0.249	0.099	112	0.055	0.023
22	0.151	0.074	70	0.654	0.260	114	0.188	0.080
23	0.577	0.282	71	0.070	0.028	116	0.300	0.127
24	0.301	0.147	72	0.015	0.006	118	0.084	0.036
26	0.142	0.070	73	0.218	0.087	119	0.038	0.016
27	0.912	0.446	74	1.218	0.485	120	0.073	0.031
29	0.312	0.152	76	0.250	0.106	122	0.237	0.116
30	0.142	0.070	77	0.356	0.151	123	0.125	0.061
32	0.214	0.104	78	0.240	0.102	124	0.308	0.151
34	0.992	0.485	79	0.751	0.318	125	0.196	0.096
36	0.453	0.221	80	0.353	0.150	126	0.364	0.178
37	0.605	0.296	81	0.700	0.297	127	0.053	0.026
38	0.188	0.092	82	0.218	0.093	128	0.187	0.091
41	0.016	0.007	83	0.610	0.258	129	0.570	0.279
43	0.295	0.125	84	0.619	0.263	130	0.089	0.044
44	0.157	0.066	86	0.135	0.057	131	0.623	0.305
45	0.861	0.365	87	1.706	0.723	132	0.792	0.387
46	1.146	0.486	88	0.688	0.291	133	0.835	0.408
47	0.657	0.279	89	0.578	0.245	134	0.623	0.305